Solid State Science and Technology, Vol. 25, No 1 (2017) 64-78
ISSN 0128-7389 | *http://journal.masshp.net*

SYNTHESIS,CHARACTERIZATION AND CATALYTIC ACTIVITY OF MODIFIED Zn- ALUMINA TOWARDS KNOEVENAGEL REACTION

Rozaina Saleh[1], and Zainab Ramli[2]

[1]*Faculty of Applied Science, Universiti Teknologi MARA, Tapah Campus, Tapah Road, 35400, Perak, Malaysia*
.
[2]*Faculty of Science, Universiti Teknologi Malaysia, 81310 Johor Bahru, Johor, Malaysia.*

Corresponding author: rozaina103@perak.uitm.edu.my

ABSTRACT

In this study, mesoporous alumina (MA) were prepared by easy and simple precipitation method using inexpensive inorganic aluminium salts with ammonium acetate (NH_4CH_3COO) as a template. A series of modified zinc-alumina was prepared by impregnation method with different %wt of Zn loading. Atomic absorption spectroscopy, energy dispersive X-ray, as well as ultraviolet-visible diffuse reflectance spectroscopy analyses proved that zinc had been successfully deposited on the surface of the modified Zn-alumina. The pyridine adsorption proved that the Zn- modified MA exhibits Lewis acidity. The reactivity of the mesoporous and modified samples were tested in the Knoevenagel condensation reaction of cinnamaldehyde with malononitrile.

Keywords: Mesoporous alumina; impregnation; knoevenagel reaction

INTRODUCTION

Aluminas are widely used as industrial catalyst and catalyst supports due to their high specific surface area [1], favorable textural properties and intrinsic acid-base characteristics [2]. With the development of large molecule hydrocarbon process, control of alumina surface area and pore size distribution had received much attention, particularly for producing high surface area mesoporous alumina with narrow pore size distribution.

The modifications of alumina have been done in several ways in order to enhance the surface properties and catalytic ability of the catalyst [3]. Zinc supported on porous material will contribute the Lewis acid sites on the surface of the catalysts. Zn-based catalysts are also very important systems for many organic reactions dealing with carbonyl species [4,5]. Most researchers reported the application of Zn-modified mesoporous alumina for many hydrocarbon reactions including hydrodesufurization

(HDS) [6], COS hydrolysis [7] and incineration of hazardous trichloroethylene (TCE) gas [8].

Knoevenagel condensation is a reaction in organic chemistry that has numerous applications in the synthesis of fine chemicals, intermediates or end-products for perfumes, pharmaceuticals and polymers. Conventionally, this reaction is catalyzed by weak bases like primary, secondary, tertiary amines under homogenous conditions [9] or by a combination of acid–base pairs in liquid phase systems [10]. The Knoevenagel reaction can also be catalyzed by homogenous Lewis acids catalyst [11-12].

In this study, a simple and easy precipitation method had been employed to synthesis mesoporous alumina by using inexpensive inorganic aluminium source. The use of solvent, pH adjustment and outside template were eliminated in this process. Aluminium acetate ($Al(CH_3COO)_3$) will be the precursor for the formation of mesoporous alumina. In this case, the acetate ion is acting as an organic template which will contribute to the formation of pores after calcination process. The synthesized mesoporous alumina was then being modified with Zn^{2+} ion by impregnation method and the characterization of all the synthesized samples were carried out. The ability of the Lewis acid sites on the modified Zn-alumina to catalyze the Knoevenagel reaction was tested in the reaction of cinnamaldehyde and malononitrile.

EXPERIMENTAL

All the chemicals used were of analytical grade. Distilled water was used throughout the experiment. Ammonium acetate (NH_4CH_3COO), aluminium nitrate nonahydrate ($Al(NO_3)_3.9H_2O$), zinc nitrate nonahydrate ($Zn(NO_3)_3.9H_2O$), cinnamaldehyde (C_9H_8O), malononitrile ($C_3H_2N_2$) and acetonitrile (CH_3CN).

Synthesis of Mesoporous Alumina

$Al(NO_3)_3.9H_2O$ (0.05 mol) was prepared in 50 mL distilled water and 11.56 g of NH_4CH_3COO was added to the solution under vigorous stirring to obtain an optically transparent and colourless solution. After 24 hours, a white precipitate was formed. An ultrasonic treatment was applied using JAC ultrasonic Cleaner (Lab Companion 1505, 370 Watt) for 30 minutes at high strength before the supernatant was removed from the precipitate by centrifugation. The precipitate was washed by distilled water for several times. Then the sample was dried in an oven at 100^{o}C for 24 hours. A portion of the sample left uncalcined and some of the sample was calcined at 650 °C. This is for the investigation of the actvation process on the reactivity of the catalyst. The sample was denoted as MA.

Synthesis of Modified Zn-Alumina

2 g of prepared MA were stirred with appropriate amount of zinc nitrate ($Zn(NO_3)_2$) with Zn/Al amount are 1%, 5% and 10%. The $Zn(NO_3)_2$ was dissolved in 3 mL distilled

water (1.5 mL per gram catalyst). The stirring process was done in room temperature for 18 hours in tightly closed container. The solution was then filtered and washed for several times. All of the synthesized samples were dried at 100°C for 24 hours. The final products were obtained by calcining the obtained white powder at 500°C for 3 hours. All samples were denoted in Table 1 below:

Table 1: Notation of the prepared samples

Samples	Description
MA	Mesoporous Alumina (calcined)
Zn/MA1	Zn/Al (1%)
Zn/MA5	Zn/Al (5%)
Zn/MA10	Zn/Al (10%)

Characterization of the Catalysts

For the analysis using Field emission scanning electron microscopy FESEM, the samples were coated with gold/titanium on respective sputter. The samples were scanned using JEOL JSM- 6330F fields emission scanning electron microscope operating at 15 kV. For the Transmission electron microscopy (TEM) analysis, the samples were prepared on 300 mesh copper grid and scanned using JEOL JEM2100 Transmittance Electron Microscope operating at 200 kV. The nitrogen adsorption-desorption measurements of calcined samples were performed using Micromeritics ASAP 2010 volumetric adsorption analyzer. The XRD pattern of all samples were recorded on Bruker Advance D8 using Siemens 5000 diffractometer with Cu Kα radiation (λ = 1.5418 Å, kV = 40, mA = 40). The powdered sample was firstly spread equally on the sample holder to form a thin and smooth layer. The sample was scanned in the 2Θ scale of 1.5° to 80° with step size 0.02° per second. Energy Dispersive X-Ray (EDX) analysis was performed using JEOL JED-2300 operating at 15 kV and Atomic Adsorption Spectroscopy (AAS) (GBC-Avanta Atomic Absorption Spectroscopy) was used in elemental analysis study. The Diffuse Reflectance UV-Visible spectroscopies (DRUV) of the solid samples were recorded on a Perkin Elmer Lambda 900 Spectrometer. About 40 mg of sample was placed in a sample holder with quartz window. After locating the sample holder in the analyzer compartment, sample was scanned in the wavelength range of 200-800 nm.

Acidity Study

For the acidity measurement, the sample was ground to a fine powder and pressed into very thin self-supporting wafer containing 10 mg cm^{-2} samples. The sample disc was

mounted in an IR cell equipped with CaF_2 windows and evacuated at 400ºC for overnight and under 10^{-4} mbar pressure. After pre-treatment, the sample was cooled to room temperature and the IR spectrum was recorded. The above sample was then exposed to 10 torr of pyridine at room temperature for 10 minutes. Desorption of pyridine was carried out by evacuating step by step for 1 hour at 100-400°C. The infrared spectra were recorded using Perkin Elmer 1600 Spectrometer with a resolution of 2 cm^{-1}. The integrated intensities of the desired bands were determined and used as a measure of the amounts of Brönsted-bound pyridine (B-py) and Lewis bound pyridine (L-py), respectively.

Catalytic Activity

Knoevenagel condensation was performed in a 25 ml round-bottomed flask fitted with reflux condenser. 16.5 mmol of cinnamaldehyde, 16.5 mmol malononitrile and 0.1 g catalyst were added to the flask. The flask was heated and refluxed for 6 hours in an oil bath at 70°C and stirred with a magnetic bar. Nitrogen gas was purged into the flask in order to avoid the oxidation of cinnamaldehyde for several minutes and the reaction system was tightly closed. After the reaction, the liquid phase was collected by centrifugation. The reaction product was quantitatively analyzed with Agilent gas chromatography with FID detector using HP-5 column (30 m length, 0.22 mm ID, and 0.11 μm film thickness).

RESULTS AND DISCUSSION

Elemental Analysis

The total zinc amount analysis was done by using Atomic Adsorption Spectroscopy (AAS) and Energy Dispersive X-Ray (EDX). The total zinc amount in each samples determined by AAS and EDX are tabulated in Table 2. From the table, we can see that the amount of zinc increased as the %wt Zn loading increased for the modified Zn-alumina samples. From the data, it can be observed that that the percent zinc amount for both analyses are the same even though the EDX analysis only detect the amount of zinc on the surface while the AAS analysis is a bulk analysis. It also can be concluded that the impregnantion method have successfully distributed zinc homogeneously on the mesoporous alumina surface. Ultraviolet-visible Diffuse Reflectance Spectroscopy (DRUV) spectra of the modified Zn- alumina samples were shown in Figure 1. The existence of the peaks after 300 nm indicates the presence of octahedral Zn^{2+} in the modified Zn-alumina samples.

Table 2: Total zinc amount determined by AAS and EDX

AAS analysis		EDX analysis
Sample	**Zinc Amount [%]**	**Zinc Amount [%]**
Zn/MA1	1	2
Zn/MA5	4	5
Zn/MA10	8	9

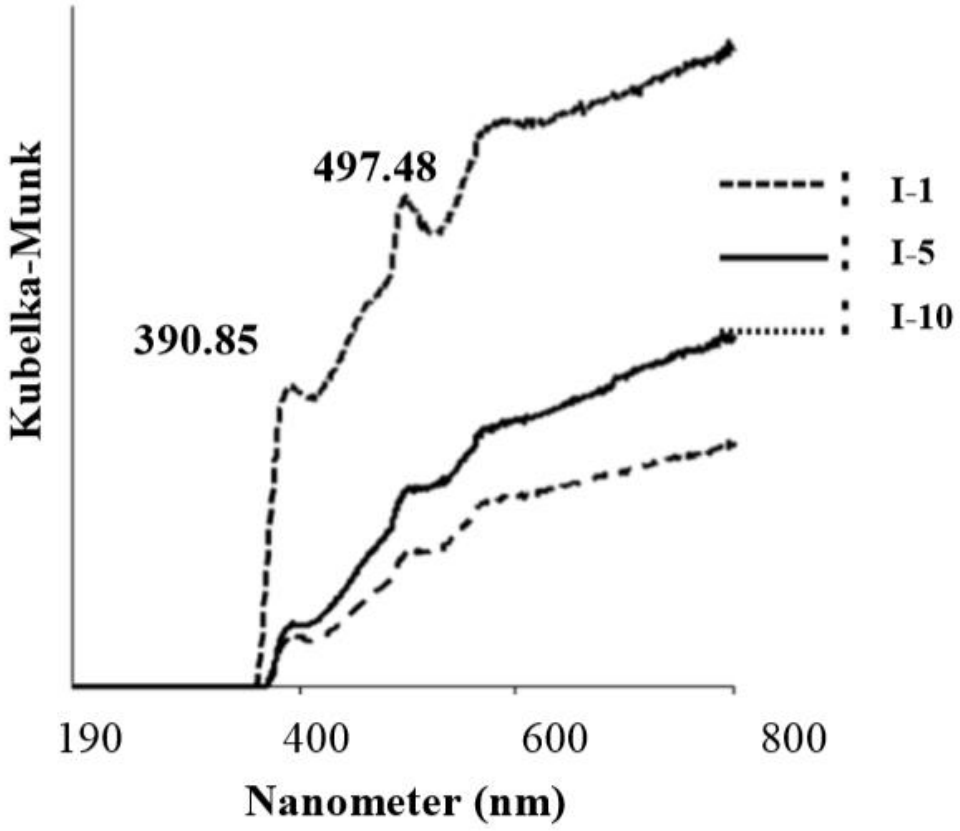

Figure 1: UV-Vis DR spectra of the modified Zn-Alumina samples

XRD diffractogram

Figure 2 shows the XRD patterns of all the synthesized samples. It is clearly seen that the mesoporous alumina and the modified Zn-alumina samples exhibit amorphous alumina and γ- alumina phase respectively. For the modified Zn-alumina samples, the crystallinity increase with the increased of the %wt Zn loading. In low angle XRD patterns for the all synthesized alumina, the intensity of the peaks increased when approaching low angle ($2q < 3°$). This indicates that the synthesized alumina have well organized pore distribution and small FWHM as claimed by other researcher [13].

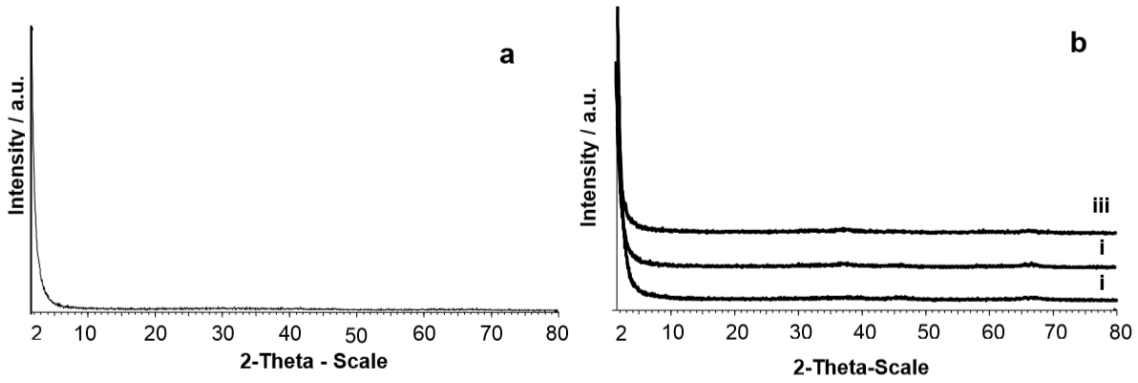

Figure 2 : XRD diffractograms of the synthesized (a) mesoporous alumina (b) Modified Zn- alumina samples (i) Zn/MA1 (ii) Zn/MA5 (iii) Zn/MA10

N_2 adsorption-desorption Measurement

The N_2 adsorption-desorption isotherms and pore size distributions curves of the synthesized alumina was shown in Figure 3. The distribution of pores was calculated from the desorption branch of the hysteresis loop using Barrett-Joyner-Halenda (BJH) method. From Figure 3a, we can see that the synthesized alumina exhibits narrow pore-size distributions with FWHM 2.5 nm centered at 6 nm. The isotherms pattern in Figure 3b showed that, the prepared mesoporous alumina present type IV isotherm, which is the characteristic of mesoporous material. The isotherms also illustrated that the sample exhibit both framework and textural porosity, with hysteresis loop started at P/P_0 ~0.5 to 1.0. The hysteresis loop at lower relative pressure is due to the framework porosity, while the steep hysteresis loop at higher relative pressure of 0.8-1.0 is caused by textural porosity. Framework porosity represents the porosity that due to the capillary condensation within the uniform mesopores, while textural porosity represents large mesopores existing in the interparticles and framework [13,14]. The isotherms also showed two steps in the hysteresis loop indicating a small amount of large mesopores exists in the samples that can be seen in the pore size distribution curves. The sample exhibits a mixture of cylinder type (H1) and stacked plane type (H3) of pores according to IUPAC classification.

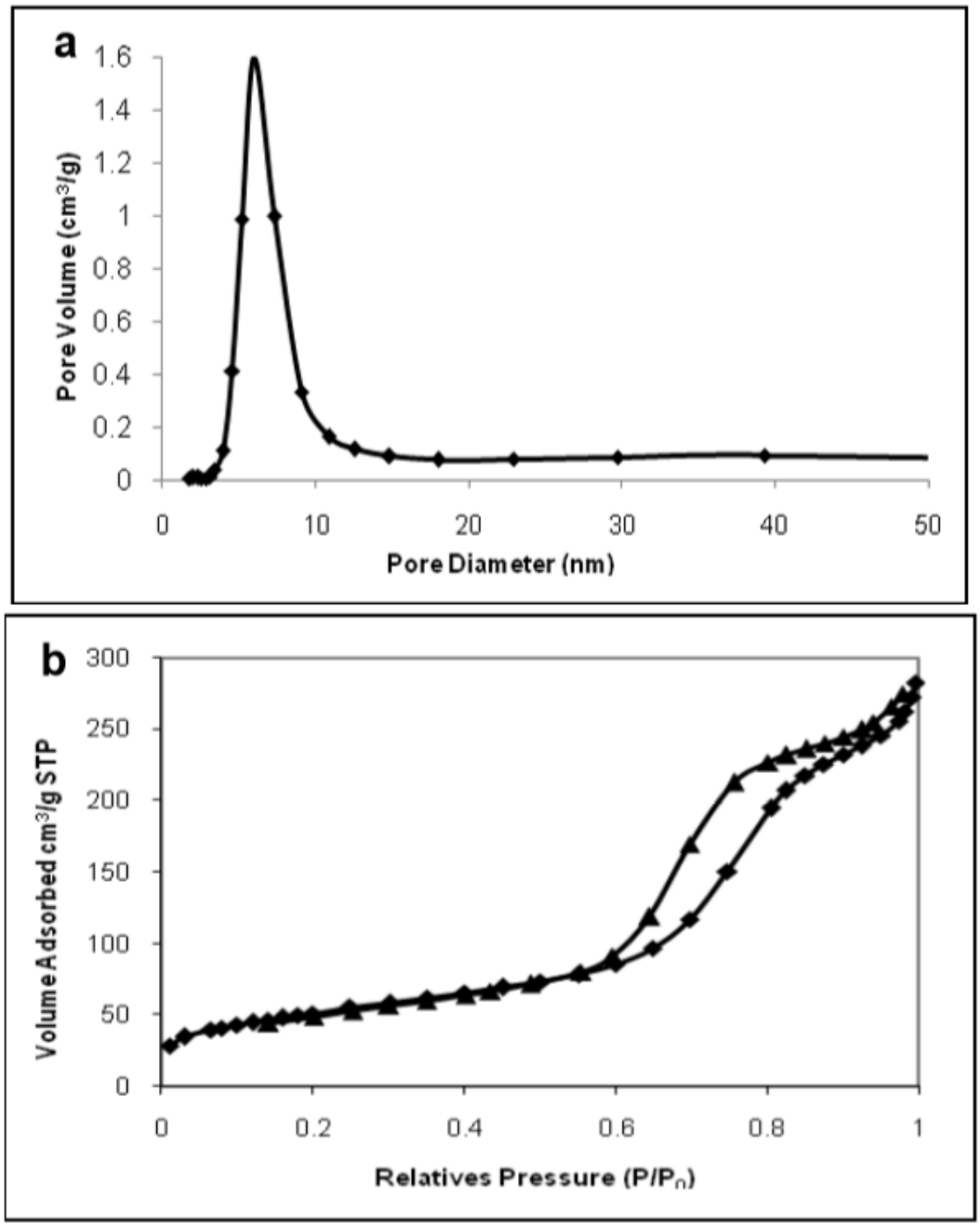

Figure 3: (a) Pore size distributions and (b) isotherm of the mesoporous alumina

Figure 4, shows the pore distribution and isotherms graphs of the modified Zn-alumina samples. From the pore distribution, it can be seen that there is no specific trend as the %wt loading zinc increased. For the 1% zinc loading (Zn/MA1), the pore distributions show no significance difference with the mesoporous alumina with FWHM centered at 2.3 nm. This could be due to only small amount of zinc is deposited on the surface of

the mesoporous alumina. Thus, the presence of the zinc does not disturb the original pore of the support. However, the pore distribution for the 5% zinc loading (Zn/MA5) transformed from single modal to bimodal pore distribution centered at 5.26 and 12.4 nm. On the other hand, the pore size distribution for 10% zinc loading (Zn/MA10) shows a bit narrower distribution compare to the mesoporous alumina support with pore centered at 1.8 nm. At 10% zinc loading, the amount of the deposited zinc is high enough to disturb the original pores that possess by the mesoporous alumina support. The pores become clogged and the pore size distribution becomes smaller and more homogeneous as compared to the mesoporous alumina support.

The isotherms of the impregnation samples show a significant difference between every %wt zinc loading. For the 1% zinc loading (Zn/MA1) the sample only consists of cylindrical type of pores while the 5% zinc loading (Zn/MA5) consist of undefined types of pores. This undefined type of pores probably leads to the bimodal pore size distribution. On the other hand, the 10% zinc loading sample (Zn/MA10) consists of the mixture of stack plane and cylindrical types of pores. All the modified Zn-alumina samples possess both framework and textural porosity, with hysteresis loop started at P/P_0 ~0.5 to 1.0.

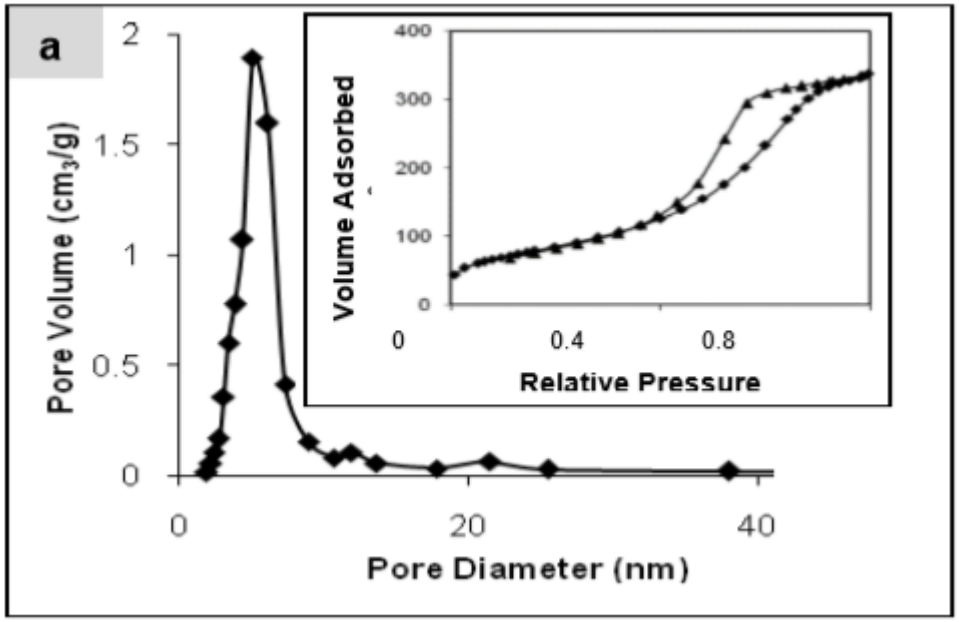

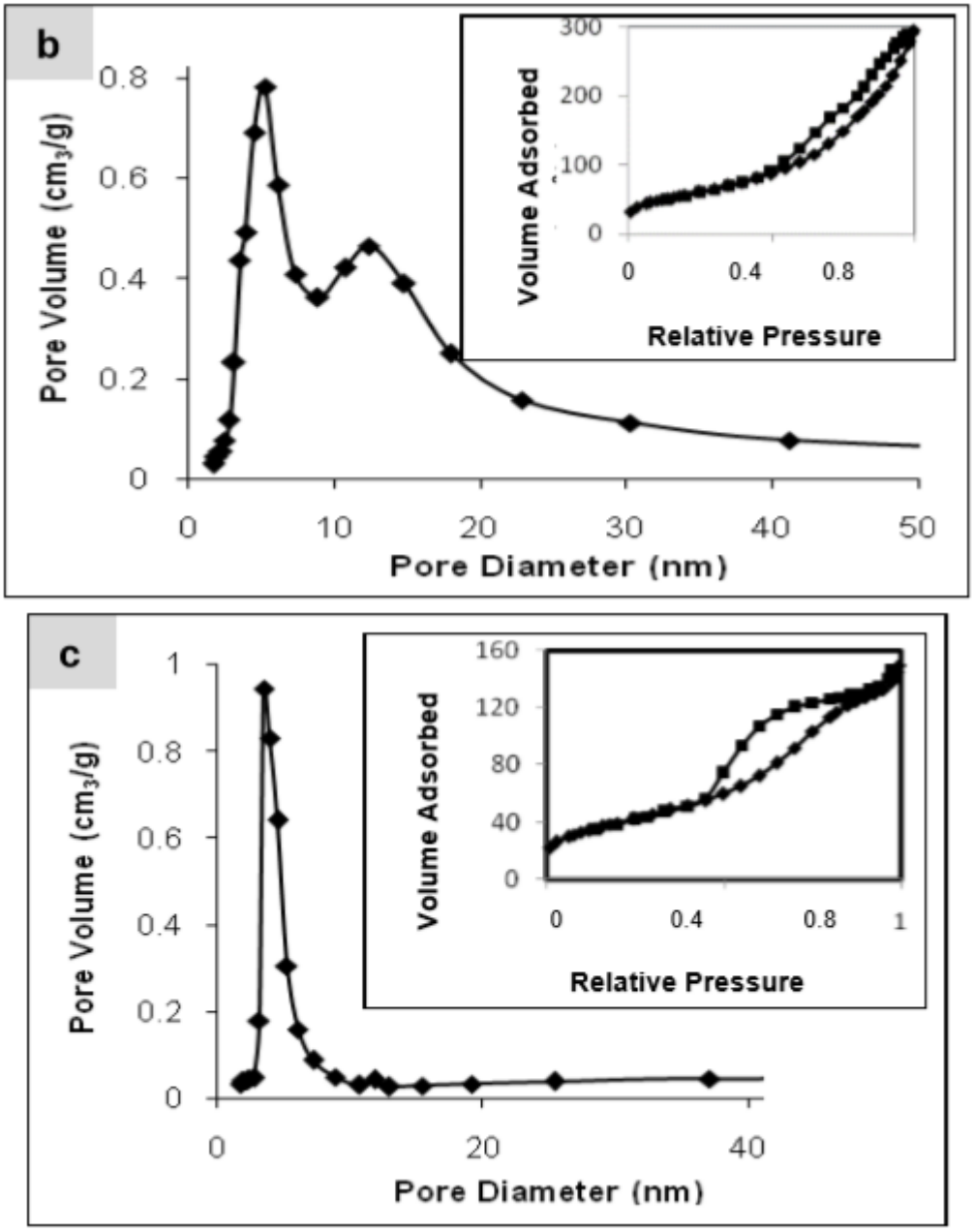

Figure 4: BJH pore-size distributions and N_2 adsorption-desorption isotherms (inset) for modified Zn-Alumina samples (a) Zn/MA1 (a) I-Zn/MA5 (c) I-Zn/MA10

Table 3 shows the BET surface area, pore volume, average pore diameter and pore size distributions of the prepared samples. The surface area of the modified Zn-alumina sample with 1% Zn loading is higher than the mesoporous alumina support. However the BET surface area decrease with the increase in the %wt zinc loading. The increase in surface area indicates that the impregnation of the zinc on the surface of the mesoporous alumina with lower zinc amount successfully deposit the zinc

homogeneously on the surface of the support. The decrease in surface area with the increase of %wt zinc loading indicates that higher loading of ZnO might obstruct the pores of the support resulting in the decrease in surface area [15].

Table 3: BET surface area, pore volume and average pore diameter of all samples

Sample	BET Surface Area [m^2/g]	Pore Volume [cm^3/g]	Average Pore Diameter [nm]
MA	202	0.4	8.5
Zn/MA1	286.70	0.53	7.1
Zn/MA5	205.92	0.46	8.2
Zn/MA10	144.82	0.23	5.8

Surface Morphology

Surface texture and morphology of the synthesized alumina were studied using Field Emission Scanning Electron Microscopy (FESEM) and Transmission Electron Microscopy (TEM). Figure 5 represents the FESEM micrograph the synthesized alumina. The sample exhibits strong agglomerated non-homogenous particles. However, the non-homogenous particles transformed to homogeneous spherical particles after impregnation process as shown in Figure 6. With the increase of %wt Zn loading, the surface of the impregnation samples become worm like particles. This observation suggests that, the amount of ZnO being adsorbed on the MA surface give effect on the surface morphology of the samples. The higher the amount of ZnO, the surface will be more worm-like structure. The FESEM micrographs of strong agglomerated samples proved that the sample exhibits textural porosity.

As shown in the TEM mocrograph in Figure 7, the mesoporous alumina consists of wormhole [16] or sponge-like in meso-range pore, indicating the advantage of a highly inter- connected pore system [13]. This result is in agreement with the data from the N_2 adsorption analysis. It is clearly shown that this mesoporous material exhibits a regular worm-like channel motif, however, without clear indication of the long-range channel packing order. Figure 7b shows the TEM micrographs of the modified Zn-alumina samples. From the micrographs, we can see that all samples have the same pore shape and also showed a slightly different pore shape with the raw mesoporous alumina.

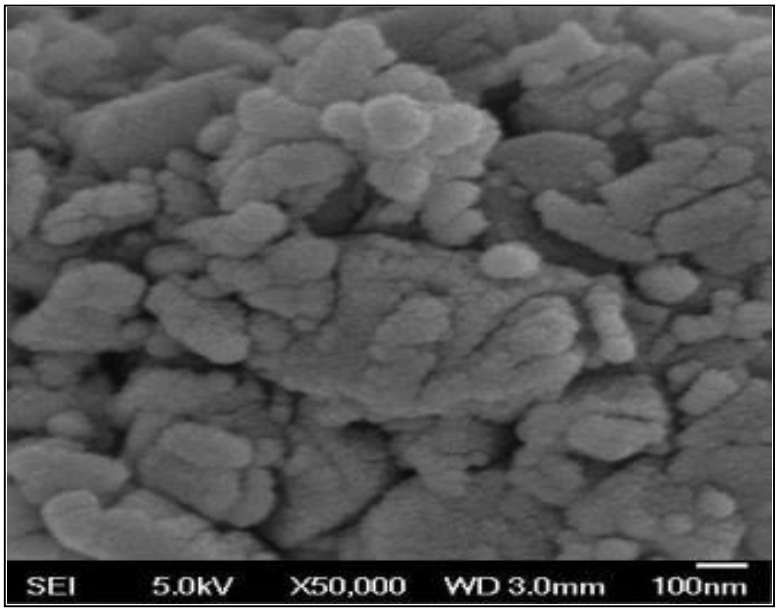

Figure 5: FESEM micrographs of the alumina sample

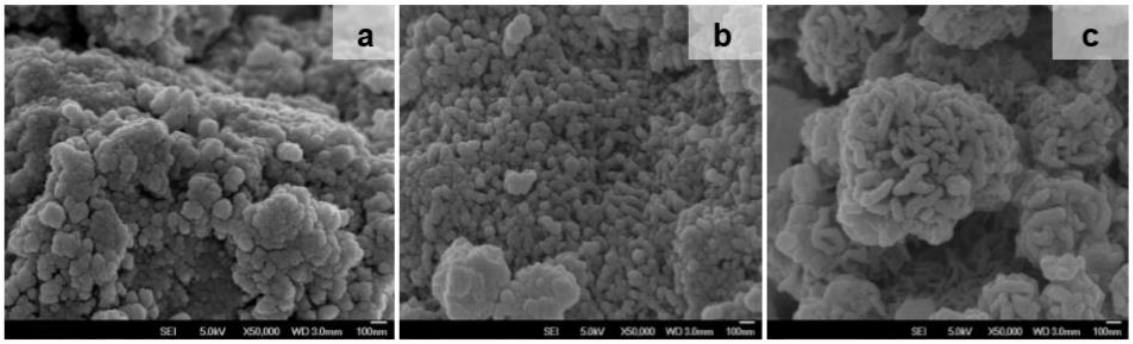

Figure 6: FESEM micrographs of the modified Zn-alumina samples (a) Zn/MA1 (b) Zn/MA5 (c) Zn/MA10

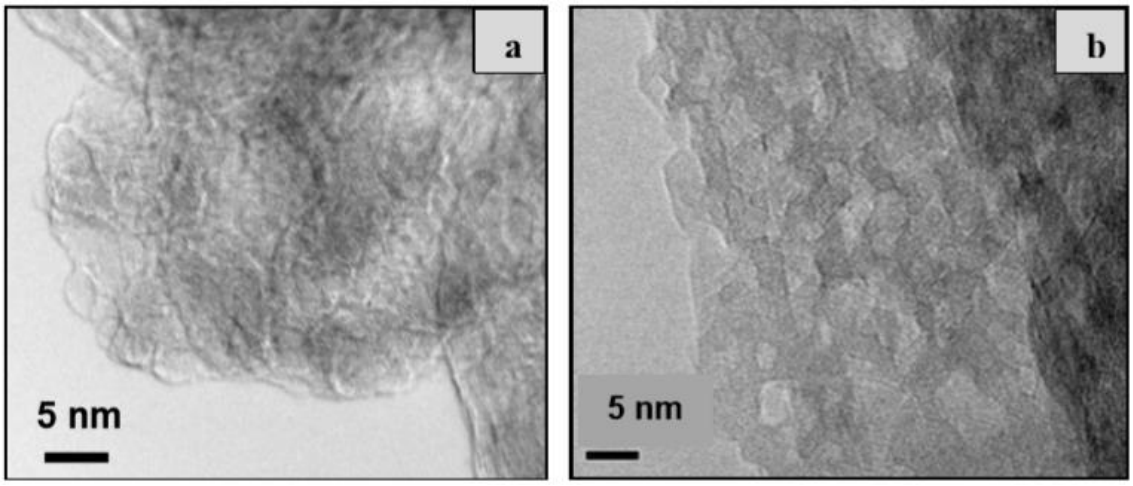

Figure 7: TEM micrographs of the (a) Mesoporous alumina (b) Modified Zn-alumina

Acidity Study

Acidity study was carried out using pyridine adsorption system and the peaks were recorded using FTIR. From the spectra in Figure 8, we can observed that all samples possess strong Lewis acid site since the Lewis acid site remain after desorption at 400 °C. Table 4 listed the integrated area at respective desorption temperature of the modified Zn-alumina samples. The integrated area is still high even after desorption at 400°C indicating strong Lewis acid side.

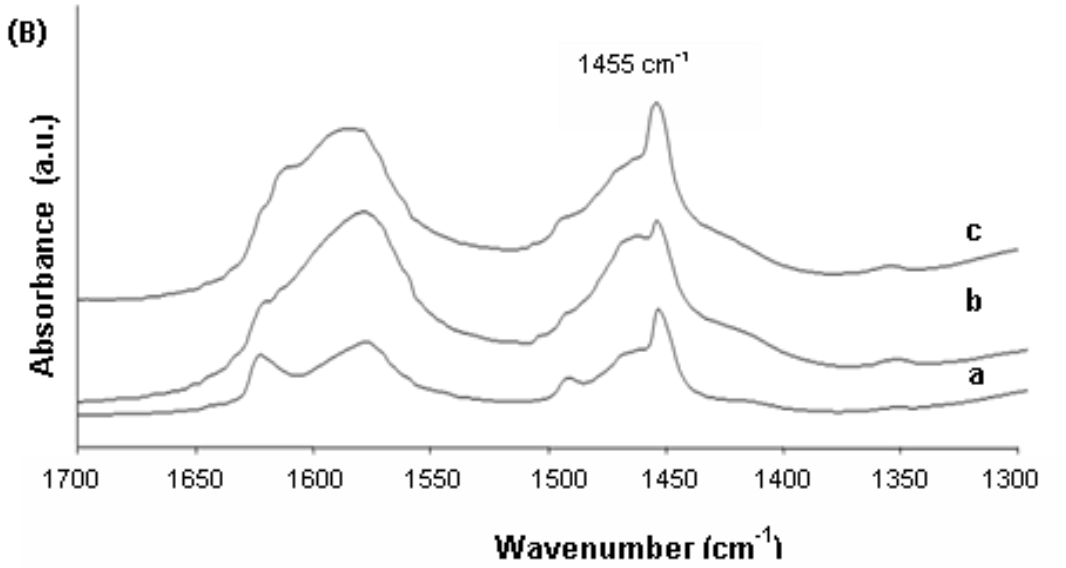

Figure 8: FTIR spectra of adsorbed pyridine on all modified Zn- Alumina samples, obtained after pyridine desorption at 400°C (i) Zn/MA1 (ii) Zn/MA5 (iii) Zn/MA10

Table 4 shows the summary of all samples with their respective pyridine adsorption region at 100°C and 400°C. It can be clearly seen that the pyridine region of the modified Zn-alumina has higher pyridine region as compared to the mesoporous alumina. This suggests that the acid sites on the modified Zn-alumina are strong and active.

Table 4: Integrated area at respective desorption temperature of the synthesized samples

Sample	Desorption Temperature	
	100°C	400°C
	Pyridine Region [A/cm^{-1}]	
MA	3.0	0.2
Zn/MA1	8.2	1.5
Zn/MA5	7.6	0.3
Zn/MA10	11.3	1.4

Catalytic Activity

The reactivity of the prepared mesoporous alumina and modified Zn-alumina to serve as a Lewis acid catalyst in Knoevenagel reaction was determined by the reaction between cinnamaldehyde with malononitrile as active methylene compound. This reaction will produce cinnamyllidenemalanonitrile as a product. The effect of activation process on the reactivity of the catalyst was investigated. From Table 5, it can be seen that generally, the activated catalysts gave slightly higher conversion as compared to the non-activated one but not so significant. This could be due to the removal of the surface hydroxyl group of the catalysts and created Lewis acid sites that are reactive for this type of reaction. The selectivity of all the catalysts still maintained with % conversion more than 85%.

Due to the high surface acidity of the Zn/MA10 sample, the sample was chosen to study the effect of reaction temperature on the reactivity of the catalyst. On the other hand, mesoporous alumina was chosen to compare the reactivity between the modified sample and its support. Table 6 shows that the reactivity of the mesoporous alumina was comparable with the Zn/MA10 sample even though mesoporous alumina has lower Lewis acidity as compared to the modified sample. It can be clearly seen that the conversion of the reactant to product increases as the temperature increase particularly for the Zn/MA10 catalyst. However after 70°C, the % conversion is actually become constant (~90%) for both catalysts. This indicates that the optimum temperature for this reaction is 70°C. On the other hand, the selectivity of the catalysts slightly decreased as the temperature increased. This could be due to the formation of side products.

Table 5: Percent conversion of the of the activated and non-activated mesoporous alumina and modified Zn-alumina

Sample	Conversion [%]	
	Non-Activated	Activated
MA	89.20	88.27
Zn/MA1	85.58	85.67
Zn/MA5	80.36	91.09
Zn/MA10	84.58	85.66

Table 6: Percent conversion of the of the activated mesoporous alumina and Zn/MA10 sample at different reaction temperature

		Conversion	Selectivity
Mesoporous Alumina	**50°C**	87.13	93.12
	70°C	88.27	89.53
	100°C	90.53	89.22
	120°C	94.76	87.86
Zn/MA10	**50°C**	65.16	92.42
	70°C	85.66	87.68
	100°C	86.67	87.91
	120°C	88.53	88.70

CONCLUSION

High surface area and narrow pore size distribution mesoporous alumina via simple precipitation method has been successfully synthesized. An attempt to impregnate Zn^{2+} ion on the surface of mesoporous alumina was successful. Most of the modified Zn-alumina samples showed a comparable pore size distribution and pore volume as compared to the mesoporous alumina. FESEM micrographs show that all modified Zn-alumina impregnation samples possess homogeneous spherical particles in nano-region. Acidity study shows that the impregnation modified samples possess high Lewis acid site. Studies on the effect of the reaction temperature showed that the reaction catalyzed by mesoporous alumina gives a comparable percent conversion as compared to

the impregnation modified samples even though mesoporous alumina has lower Lewis acidity as compared to the modified sample. This suggests that the Lewis acid sites alone will not actively contribute to the catalytic activity of the catalyst. The combination of the high surface area, well organized pore distribution and high Lewis acidity are the criteria of the catalyst that will be highly active in the Knoevenagel reaction between cinnamaldehyde and malononitrile to produce cinnamyllidenemalanonitrile

REFERENCES

[1] Z. Gan, G. Ning, Y. Lin, and Y. Cong, *Mater. Lett.* **61** 3758- 3761 (2007)
[2] Q. Liu, A.Wang, X.Wang, and T. Zhang, *Microporous Mesoporous Mater.*, **100** 35-44 (2007)
[3] A. Tarlani and M.P. Zarabadi, *Solid State Science* **16** 76-80 (2013)
[4] J.S. Albero, J.C.S. Ruiz, A.S. Escribano, and F.R. Reinoso, *Appl. Catal. A.* **292** 244-251 (2005)
[5] W. Lu, G. Lu, Y. Luo and A. Chen, *J. Mol. Catal. A: Chem.* **188** 225-231 (2002)
[6] J. Trawezyński, A. Kubacki, J. Wrzyszez, M. Zawdzki, H. Grabowska and W. Miśta, *React. Kinet. Catal. Lett.* **76** 259-264 (2002)
[7] H. Huang, N. Young, B.P. William, S.H. Taylor, and G. Hutching, *Catal. Lett.* **104** 17-21 (2005)
[8] J.C Chen and C.T Tang, *J. Hazard. Mater.* **142** 88-96 (2007)
[9] Y. Goa, P. Wu, and T. Tatsumi, *J. Catal.* **224** 107-114 (2004)
[10] M.J. Climent, A. Corma, V. Fornés, A. Frau, R.G. López, S. Iborra, and J. Primo, *J. Catal.* **163** 392- 398 (1996)
[11] J.R. Harjani, S.J. Nara, and M. Salunkhe, Lewis *Tetrahedron Lett.* **43** 1127-1130 (2002)
[12] P.A Clarke, and W.H.C.Martin, *Org. Lett.* **4** (25) 4527-4529 (2002)
[13] Y. Kim, C. Kim, P. Kim, P. Yi, *J. Non. Crys. Sol*. **351** 550-556 (2005)
[14] Q.Liu, A.Wang, X. Wang and T.Zhang, *Micropor. Mesopor. Mater.* **92** 10-21 (2006)
[15] W. Lu, G. Lu, Y. Luo, and A. Chen, *J. Mol. Catal. A: Chem.,* **188** 225-231 (2002)
[16] N. Žilkova, A. Zukal and J.Čejka, *Micropor. Mesopor. Mater.,* **95** 176-179 (2006)